

Predictive load accommodation in a micro-grid

Ashish Laddha¹, Satyanarayana Neeli¹, Vijayakumar Krishnasamy²

¹Department of Electrical Engineering, Malaviya National Institute of Technology, Jaipur, India

²School of Electrical and Computer Engineering, Indian Institute of Information Technology, Design and Manufacturing, Kancheepuram, India

Article Info

Article history:

Received Mar 26, 2022

Revised Sep 27, 2022

Accepted Oct 15, 2022

Keywords:

Four-port dc/dc converter
Improved cyclic averaged current
Model prediction-based control
Renewable power generating resources
Variable ac-natured load

ABSTRACT

This manuscript applies model prediction-based control (MPC) to accommodate the variable ac-natured load (AL) by optimally allocating the fuel cell (FC), battery, solar photovoltaic (SP) power in a four-port dc/dc converter (FPDDC). The presented work considers the FC, battery, SP, and AL at the first, second, third, and fourth ports of the FPDDC, respectively. The small signaled state-space representation of the FPDDC has been obtained through the improved cyclic averaged current. Then, to get the receding horizon-based MPC optimal control action, $\Delta u^* [k]; k = 0, 1, 2, 3, \dots$, the above-mentioned model of the FPDDC is discretized. The $\Delta u^* [k]$ has been obtained by formulating a performance index, $J_a [k]$ based on an error minimization between the reference AL power demand, $r_{pd} [k]$ and the actual AL power, $y [k]$. The corresponding results have been obtained through the Simulink platform of the MATLAB. Further, the article takes sequential quadratic programming (SQP) into consideration to benchmark these solutions.

This is an open access article under the [CC BY-SA](https://creativecommons.org/licenses/by-sa/4.0/) license.



Corresponding Author:

Ashish Laddha

Research Scholar,

Department of Electrical Engineering, Malaviya National Institute of Technology,

Jaipur, Rajasthan-302017, India

Email: 2016ree9538@mnit.ac.in

1. INTRODUCTION

In today's power system, renewable power generating resources (RPGRs) are important to meet the variable power demand of ac-natured load (AL). Hybridized RPGRs along with energy-storing device(s) by formulating a micro-grid [1] result in flexible, reliable, and cost-effective power that can cope with the load demand [2], [3]. Further, optimal allocation of available RPGRs [4] is desirable in such a system that involves challenges at the integration, allocation, and control levels. This challenge further attains complexity if the network involves RPGR(s) considering the natural intermittent behavior of the latter. This intermittent behavior further gets reflected in the generating voltages of the RPGRs. Moreover, in a power network, voltage across the RPGRs, energy-storing device(s), and AL may not always be similar. Power electronic interfacing arrangements like dc/dc converters find appropriateness in this regard. Multiple input and output-based multi-port dc/dc converter (MPDDC) possesses several advantages over the single input and output-led dc/dc converter [3], [5] and references there in. However, many of the investigations on the MPDDC mainly concentrated on topological, utilized devices, efficacy, and operating conditions aspects.

Whereas, controlling [6] systems having the RPGRs and power conversion device(s) is a challenging task because of the inherent non-linearity of the two. This control further attains complexity due to the uncertain nature of the RPGRs and unavailability of the complete state vector. Thus, state-based control techniques

become practically inapplicable due to this unavailability. Hence, the output of the system has to be utilized to realize the control action. The main drawback of the output feedback is that it cannot realize any arbitrary control law. An observer [7]-[9] overcomes this drawback by estimating the unknown states of systems but enhances the dimension of the latter and is uneconomic. Well known controllers like proportional integral [10]/proportional integral derivative [11], [12] also don't find appropriateness to control the multiple input and output systems. This necessitates exploring suitable control technique(s) for such systems. Model prediction-led control (MPC) [13]-[18] has widely been employed in industries, as well as RPGRs-converter systems due to the possibility of control action modification at the intermediate level(s), online optimization, systematic method to assign specific weights to control inputs, simpler implementation, and capability to deal with multiple variables, constraints, and non-linearity [19]-[21]. Digital computing devices and interfacing hardware, lesser board-space requirement, supportive price (due to single-chip integrated multiple control functioning), and programming facility have popularized the digitalized control [22] of dc/dc converters. Hence, the implementation of the MPC schemes in their digitalized form is preferable over the analogue form. The MPC provides the solution in the receding horizon manner at each sampling instant, $k = 0, 1, 2, 3, \dots$ by optimizing the formulated cost-functional, $J_a[k]$ over a prediction-horizon, n_p including the constraints. Further, at each k , a finite set of control actions for a particular control-horizon, n_c ($n_c \leq n_p$) needs to be computed. Afterward, the first control action is only applied to the system as per the receding horizon philosophy.

This communique obtains improved cyclic averaged current-led large and small signaled responses of the chosen power in a four-port dc/dc converter (FPDDC) states. Afterward, it discretizes the small signaled state-space representation of the FPDDC. Later, the brief applies the MPC to accommodate the AL with optimally allocated fuel cell (FC), battery [2], and solar photovoltaic (SP) generations. For the validation of the obtained results, the paper considers the sequential quadratic programming (SQP) discussed in [5] and references there in. The SQP has been utilized to optimize nonlinear systems like the FPDDC including the constraints. Besides, it provides the assurance of getting the feasible starting point as required for the optimization.

2. MODELING OF THE INVESTIGATED SYSTEM

Figure 1 provides the pictorial representation of the studied FPDDC. Here, L_m and C_m denote the filter inductor and filter capacitor of the low-pass filter at a port m ; $\forall m = 1, \dots, 4$, respectively. The charge controller at the battery port (i.e., the port two) regulates the charging, as well as discharging current of the battery. The reverse-directional power flow at the SP port (i.e., the port three) is preventable by utilizing a diode, D , subsequent to the SP system.

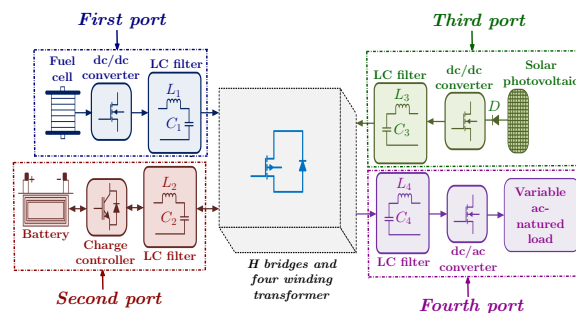


Figure 1. Schematic of the investigated FPDDC

The dc/ac converter before the AL transforms the filtered dc power to the ac form. Phase angles (i.e., control inputs) between any two ports m and n (i.e., $\phi_{mn} = \phi_n - \phi_m$; $\forall n = 1, \dots, 4$; $m \neq n$) manage the power flow within the FPDDC. The modified periodic-natured cyclic averaged current [3] has been considered to model the FPDDC of the Figure 1. The linearized expressions of the FPDDC, here, have been obtained around the *quiescent point* (I_m, V_n , and ϕ_{mn}) [3]. Based on these expressions, the continuous time state-space representation of the FPDDC while accommodating the disturbances is as mentioned by (1).

$$\begin{aligned} \dot{x}(t) &= A_c x(t) + B_c u(t) + D_c w(t) \\ y(t) &= C x(t) \end{aligned} \quad (1)$$

Where $x(t) = [v_1(t), v_2(t), v_3(t), v_4(t), i_1(t), i_2(t), i_3(t)]^T \in \mathbb{R}^7$, $u(t) = [\phi_{21}(t), \phi_{23}(t), \phi_{24}(t)]^T \in \mathbb{R}^3$, and $w(t) = [i_4(t), v_{i,1}(t), v_{i,2}(t)]^T \in \mathbb{R}^3$ are the *state*, *control input*, and *disturbance* vectors of the FPDDC, respectively. Whereas the currents $i_o(t)$; $\forall o = 1, \dots, 3$ constitute the measured output vector of the studied interface. Here, $i_{1,2,3,4}(t)$ and $v_{1,2,3,4}(t)$ account for the current and voltage at the FC, battery, SP, and AL ports of the interface, respectively. $\phi_{21}(t)$, $\phi_{23}(t)$, and $\phi_{24}(t)$ denote the phase angles between the battery and FC ports, battery and SP ports, and battery and AL ports of the FPDDC, respectively. Real-valued system matrices A_c , B_c , D_c , and C of the FPDDC are as provided in [3]. For the rated value (i.e., 1 p.u.) of the voltage at each port, the output vector of the FPDDC is composed of $y_1(t) = p_{FC}(t)$, $y_2(t) = p_{BAT}(t)$, and $y_3(t) = p_{SP}(t)$. Discretization of the FPDDC model in (1) is necessary for applying the MPC-based control action. Zero-order hold-driven discrete time representation of the FPDDC, by considering the sampling period, T_s and the denotation $x[k]$ for the $x[kT_s]$, is as per the subsequent expression.

$$\begin{aligned} x[k+1] &= \Phi_d x[k] + \Gamma_d u[k] + D_d w[k] \\ y[k] &= Cx[k] \end{aligned} \quad (2)$$

Where the expressions of the system matrix Φ_d , control input matrix Γ_d , and disturbance matrix D_d of the discretized FPDDC are $e^{A_c T_s}$, $\int_0^{T_s} e^{A_c \tau} B_c d\tau$, and $\int_0^{T_s} e^{A_c \tau} D_c d\tau$, respectively.

3. RESEARCH METHOD

MPC is used to design a controller that minimizes the system output signal's deviations from the *reference* signal with the minimal control effort. Application of the full control action may bring the actuator in the saturation state. Whereas, applying control in *incremental* manner [23] is free from this issue, enhances the robustness, and does not demand much knowledge of system parameters. Hence, this work proceeds with the incremental model of the FPDDC (2) in the following manner.

$$\begin{aligned} \Delta x[k+1] &= \Phi_d \Delta x[k] + \Gamma_d \Delta u[k] + D_d \Delta w[k] \\ y[k] &= C \Delta x[k] + y[k-1] \end{aligned} \quad (3)$$

Where $\Delta x[k]$, $\Delta u[k]$, and $\Delta w[k]$ indicate increment vectors in the state, control input, and disturbance, respectively. The corresponding expressions of these vectors are $x[k] - x[k-1]$, $u[k] - u[k-1]$, and $w[k] - w[k-1]$, respectively. Here, the MPC-based control action for the FPDDC model (3) has been designed by considering $\Delta u[k+\gamma] = 0$; $\forall \gamma = n_c, \dots, n_p$. This helps in the minimization of the controlling effort. The *predicted state vector* for the system (3) is obtainable by considering that the disturbance vector does not change over the n_p from its value at the k th sampling time instant, i.e., $\Delta w[k+\gamma] = 0$; $\forall \gamma = 1, \dots, n_p$ [24]. Predicted output vector of the system (2) is computed by multiplying the predicted state expressions with the matrix C as $y[k+\gamma|k] = Cx[k+\gamma|k]$; $\forall \gamma = 1, 2, 3, \dots, n_p$. A cost-functional, $J[k]$, in (4), has been formulated to drive the system predicted output, $y[k]$ to its reference value, $r_{pd}[k]$ from the current discrete time step k over the n_p .

$$J[k] = \underset{U_k}{\operatorname{argmin}} \left(\sum_{\gamma=1}^{n_p} \|r_{pd}[k+\gamma|k] - y[k+\gamma|k]\|_{Q_1^2} + \sum_{j=1}^{n_c} \|\Delta u[k+j-1|k]\|_{R_1^2} \right) \quad (4)$$

Where $Q_1 \in \mathbb{R}^{\alpha \times \alpha}$ ($R_1 \in \mathbb{R}^{\beta \times \beta}$) is a *positive semi-definite* (*positive definite*) matrix. The α and β , here, represent the number of output and input variables, respectively. The *second-norm* and the *weighted-norm* of the x are denoted by $\|x\|$ and $\|x\|_T$, respectively. On defining Y_p and ΔU_k as (5).

$$\begin{aligned} Y_p &\stackrel{\text{def}}{=} [y[k+1|k], \dots, y[k+n_c|k], \dots, y[k+n_p|k]] \ \& \\ \Delta U_k &\stackrel{\text{def}}{=} [\Delta u[k], \Delta u[k+1|k], \dots, \Delta u[k+n_c-1|k]] \end{aligned} \quad (5)$$

The expression of predicted output is rewritable as $Y_p = M \Delta x[k] + \Psi \Delta U_k + \zeta y[k] + \Gamma \Delta w[k]$. Here, the matrices M , Ψ , ζ , and Γ are determined from the matrices Φ_d , Γ_d , C , and D_d of the (2) and predicted output

expression. Using the expressions of the Y_p and ΔU_k as per the (5) and reproduced predicted output, the cost-functional (4) is $J[k] = (R_{pd} - Y_p)^T Q (R_{pd} - Y_p) + \Delta U_k^T R \Delta U_k$. Here, $Q \in \mathbb{R}^{n_p \alpha \times n_p \alpha}$ ($R \in \mathbb{R}^{n_c \beta \times n_c \beta}$) is a *positive semi-definite* (*positive definite*) diagonal matrix. Q_1 and R_1 indicate the diagonal elements of the matrices Q and R , respectively and the $R_{pd} = [r_{pd}[k+1], r_{pd}[k+2], \dots, r_{pd}[k+n_p]]^T$. The MPC-led optimization with respect to the sampling time instants is of the form:

$$\begin{aligned} J_a[k] &= \arg \min_{\Delta U_k} J[k] & (6) \\ \text{s. t. } p_{FC}[k] + p_{BAT}[k] + p_{SP}[k] &= r_{pd}[k] \\ 0 \leq p_{FC}[k] &\leq ic_{FCmax} \\ 0 \leq p_{SP}[k] &\leq ic_{SPmax} \\ -ic_{BATmin} \leq p_{BAT}[k] &\leq ic_{BATmax} \\ \Delta x_{[k+i|k]} &= f(\Delta x_k, \Delta U_k) \end{aligned}$$

where $p_{FC}[k]$, $p_{BAT}[k]$, and $p_{SP}[k]$ indicate the powers generated from the FC, battery, and SP at the k th sampling instant, respectively. $ic_{(FC,BAT,SP)max}$ and ic_{BATmin} are the maximum installed capacity of the FC, battery, and SP and minimum installed capacity of the battery, respectively. The first expression of the constraints is to ensure an equality between the total generation and the demand at every sampling instant, k . Moreover, $\Delta x_{[0|k]} = [0, 0, 0, 0, 0, 0, 0]^T$ denotes the *initial* condition of the system. The optimal global solution, given in the (7), is obtained by setting the gradient of the cost-functional to the optimization variable vector equal to zero.

$$\Delta U_k^* = (\Psi^T Q \Psi + R)^{-1} \Psi^T Q (R_{pd} - M \Delta x[k] - \zeta y[k]) - \Gamma \Delta w[k] \quad (7)$$

Where ΔU_k^* stands for the optimal control sequence over the n_c . The receding horizon policy makes the expression $\Delta u^*[k] = [1, 0, 0, \dots, 0] \Delta U_k^*$ to hold at the k th sampling instant. Here, the U_k^* is expressible as $(\Psi^T Q \Psi + R)^{-1} \Psi^T Q (R_{pd} - M \hat{x}[k] - \zeta y_s[k])$. The term $[1, 0, 0, \dots, 0]$ denotes the gain, K_{MPC} of the MPC-based control action. Figure 2 shows the FPDDC system as implemented in the MATLAB's Simulink. Here, the 'Conn 1' along with the 'Conn 2' represents the simulative connections. The implementation of the AL (to be accommodated through the MPC-led control) takes place as per Figure 3. The same for the FC, battery, and SP has been skipped here due to the space limitation.

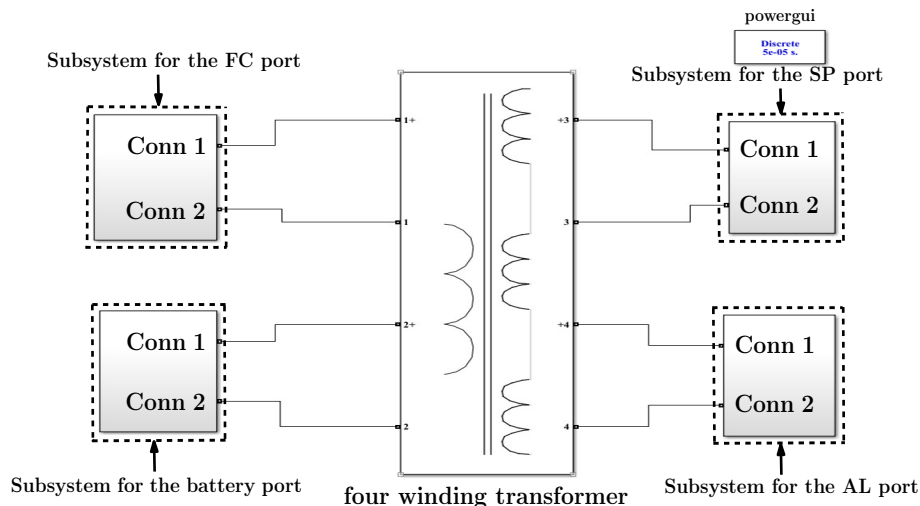


Figure 2. Implementation of the FPDDC in the Simulink platform

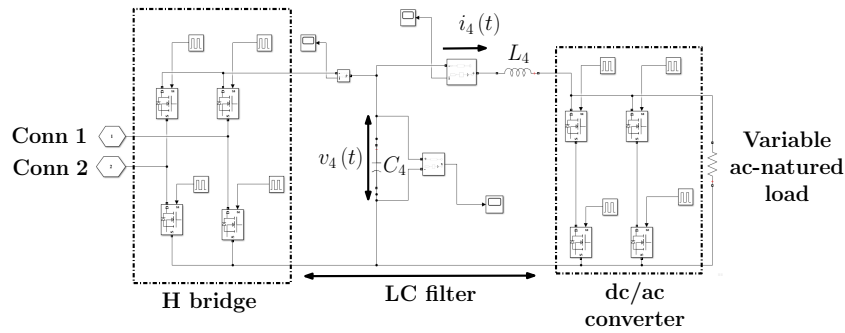


Figure 3. Implementation of the AL port in the Simulink platform

4. RESULTS AND DISCUSSION

The inter-port reactances (in p.u.) between the FC and battery ports, FC and SP ports, FC and AL ports, battery and SP ports, battery and AL ports, and SP and AL ports are 0.6004, 0.3002, 0.8006, 0.3753, 1.0007, and 0.5004, respectively. The MPC-driven control, with $n_p = 10$ and $n_c = 3$, aims to accommodate the AL (2400 W, 230 V) through optimally allocated generations of the FC (1500 W, 24 V), battery (150 W, 48 V), and SP (750 W, 24 V). The inductances (in mH) of the corresponding filtering circuits are 0.5654, 0.5497, 0.0832, and 0.1146, respectively. Whereas, the respective capacitances (in mF) of the same are 0.0063, 0.0072, 0.0757, and 0.0530. The switches at the four ports of the FPDDC operate at 20 kHz.

The optimal values of the phase shifts $\phi_{21} [k]$, $\phi_{23} [k]$, and $\phi_{24} [k]$ have been obtained as -22.62 , -36.51 , and -4.01 radian ($\times 10^{-2}$), respectively. The article illustrates the comparison of the large signal responses (LSRs) and small signal responses (SSRs) in view of the state variables $i_2(t)$ and $v_3(t)$. Figures 4 and 5 depict the LSRs and SSRs for the $i_2(t)$ (current flowing through the filter inductor at the battery port) and $v_3(t)$ (voltage across the filter capacitor of the SP port), respectively. It is noticeable that the SSR trajectories almost match with the corresponding LSR curves. Further, quarter an hour power demand of a hospital premise [25] in India has been taken as the reference, $r_{pd} [k]$.

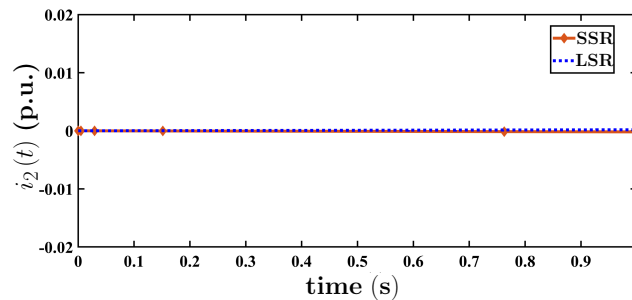


Figure 4. LSR and SSR responses for the filter inductor current at the battery port

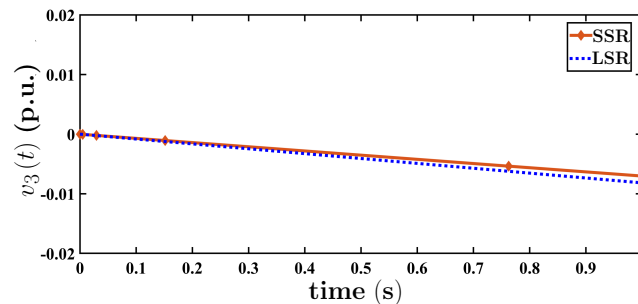


Figure 5. LSR and SSR responses for the filter capacitor voltage at the SP port

Figure 6 depicts the tracking of the $r_{pd}[k]$ by utilizing the control strategies of the MPC, $y_{MPC}[k]$ and SQP, $y_{SQP}[k]$. Figure 7 portrays the tracking errors corresponding to the MPC, $e_{y_{MPC}}[k]$ and SQP, $e_{y_{SQP}}[k]$ approaches. It is observable from the Figure 7 that the *optimal control sequence of the receding horizon-based MPC* makes $e_{y_{MPC}}[k] < e_{y_{SQP}}[k]$ to hold. Furthermore, the $r_{pd}[k]$ is accommodated through optimal allocation of the $p_{FC}[k]$, $p_{BAT}[k]$, and $p_{SP}[k]$ according to Figure 8. To this end, the availability of the $p_{FC}[k]$, $p_{BAT}[k]$, and $p_{SP}[k]$ is 1st-96th, 1st-96th, and 29th-68th instants on an arbitrary day, respectively. Furthermore, the negative $ic_{p_{BAT_{min}}}$ of -150 W capacity corresponds to the battery's charging operation.

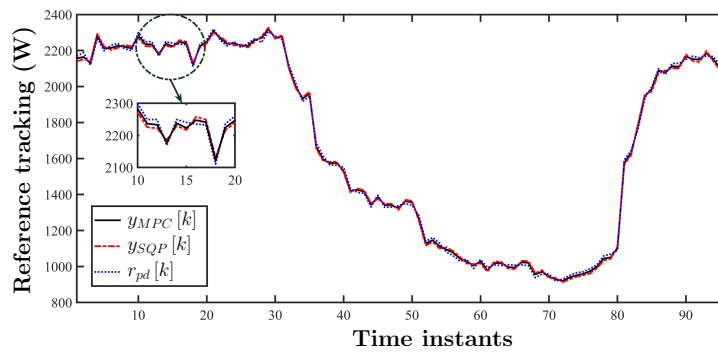


Figure 6. Reference power tracking with the MPC and SQP-driven control schemes

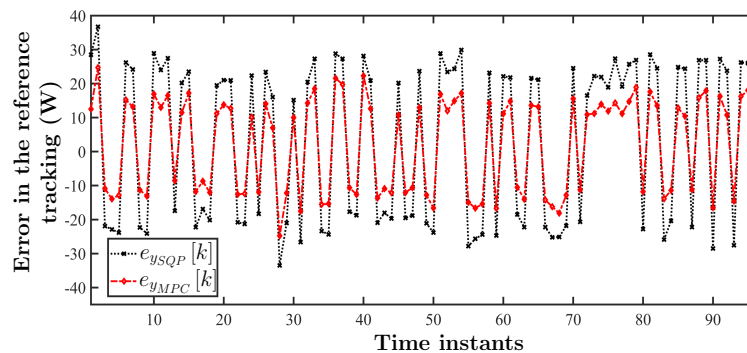


Figure 7. Comparison of the tracking errors corresponding to the MPC and SQP

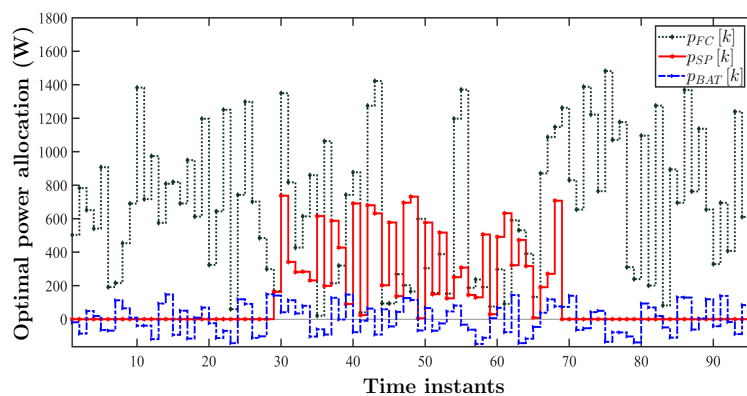


Figure 8. Optimal generations in the micro-grid while accommodating the AL

5. CONCLUSION

The small signaled continuous time state-space representation of the studied FPDDC has been obtained according to the improved cyclic averaged current. The term $w(t)$ in the aforesaid modeling indicates the disturbances corresponding to the power generating resources and continuously changing AL. The matching LSRs and SSRs of the considered states of the FPDDC suggest that adopting the small signal analysis minimizes the computational efforts. Subsequently, the zero-order hold-led discretization enabled to get the MPC-based optimal inter-port phase angle values. These phase angles enable the accommodation of the AL via optimally allocated FC, battery, and SP generations. The simulative outcomes provide the confirmation regarding the effectiveness of the MPC-driven control. In addition, the comparison of these results with the SQP approach reveals the supremacy of the MPC.

ACKNOWLEDGEMENTS

Authors express their gratitude to the Science and Engineering Research Board (SERB), Department of Science and Technology (DST), GoI regarding monetary assistance provided to the project entitled "Optimal output sample based control of multiport DC-DC converters" (ECR/2017/000968/ES).





REFERENCES

- [1] E. A. Molina-Viloria, J. E. C. Becerra, and F. E. H. Velasco, "Reactive power sharing in microgrid using virtual voltage," *International Journal of Electrical Computer Engineering (IJECE)*, vol. 11, no. 4, pp. 2743-2751, Aug. 2021, doi: 10.11591/ijece.v11i4.pp2743-2751.
- [2] I. S. B. Hburi, H. Al Khazaali, O. Bayat, and N. H. A. S. Atab, "Maximum power point tracking control for wind turbines with battery storage system," *TELKOMNIKA (Telecommunication Computing Electronics and Control)*, vol. 19, no. 2, pp. 564-574, Apr. 2021, doi: 10.12928/TELKOMNIKA.v19i2.16346.
- [3] A. Laddha, N. Satyanarayana, and R. Jain, "Modeling and analysis of four-port DC-DC converter," *2019 International Conference on Power Electronics, Control and Automation (ICPECA)*, 2019, pp. 1-6, doi: 10.1109/ICPECA47973.2019.8975534
- [4] M. Yang, Y. Cui, and J. Wang, "Multi-Objective optimal scheduling of island microgrids considering the uncertainty of renewable energy output," *International Journal of Electrical Power & Energy Systems*, vol. 144, p. 108619, Jan. 2023, doi: 10.1016/j.ijepes.2022.108619.
- [5] A. M. Ari, L. Li, and O. Wasynczuk, "Control and optimization of N -port DC-DC converters," in *IEEE Transactions on Control Systems Technology*, vol. 24, no. 4, pp. 1521-1528, Jul. 2016, doi: 10.1109/TCST.2015.2495236.
- [6] D. M. Narasimhaiah, C. K. Narayanappa, and G. S. Lakshmaiah, "Hybrid controller design using gain scheduling approach for compressor systems," *International Journal of Electrical and Computer Engineering (IJECE)*, vol. 12, no. 3, pp. 3051-3060, Jun. 2022, doi: 10.11591/ijece.v12i3.pp3051-3060.
- [7] M. Shakarami and K. Esfandiari, "Rapid fault reconstruction using a bank of sliding mode observers," *Journal of the Franklin Institute*, Sep. 2022, doi: 10.1016/j.jfranklin.2022.09.012.
- [8] P. Bernard, V. Andrieu, and D. Astolfi, "Observer design for continuous-time dynamical systems," *Annual Reviews in Control*, vol. 53, pp. 224-248, Jan. 2022, doi: 10.1016/j.arcontrol.2021.11.002.
- [9] I. Daldoul and A. S. Tlili, "Secured transmission design schemes based on chaotic synchronization and optimal high gain observers," *Simulation Modelling Practice and Theory*, vol. 120, p. 102625, Nov. 2022, doi: 10.1016/j.simpat.2022.102625.
- [10] A. Al-Qallaf and K. El-Sankary, "Design of time-mode PI controller for switched-capacitor DC/DC converter using differential evolution algorithm-A design methodology," in *IEEE Transactions on Computer-Aided Design of Integrated Circuits and Systems*, Feb. 2022, doi: 10.1109/TCAD.2022.3149850.
- [11] A. Laddha, N. Satyanarayana, and B. P. Sanvat, "Design of PID and model predictive control for stabilization of photovoltaic voltage," *2020 IEEE International Conference on Power Electronics, Drives and Energy Systems (PEDES)*, 2020, pp. 1-6, doi: 10.1109/PEDES49360.2020.9379370.
- [12] A. Houari, I. Bachir, D. K. Mohamed, and M. K. Mohamed, "PID vs LQR controller for tilt rotor airplane," *International Journal of Electrical and Computer Engineering (IJECE)*, vol. 10, no. 6, pp. 6309-6318, Dec. 2020, doi: 10.11591/ijece.v10i6.pp6309-6318.
- [13] H. S. Lee, and P. Park, "Implementation of control structure for steel pickling process using model predictive controller," *IFAC-PapersOnLine*, vol. 55, no. 7, pp. 679-684, Jan. 2022, doi: 10.1016/j.ifacol.2022.07.522.
- [14] S. Chen, J. L. Mathieu, and P. Seiler, "Stochastic model predictive controller for wind farm frequency regulation in waked conditions," *Electric Power Systems Research*, vol. 211, p. 108543, Oct. 2022, doi: 10.1016/j.epsr.2022.108543.
- [15] Y. Fang, M. Fei, H. Qian, L. Wang, and K. Chen, "Nuclear reactor power level model predictive control: a consideration of coolant outlet temperature relaxation tracking method," *Nuclear Science and Engineering*, vol. 196, no. 7, pp. 886-898, Mar. 2022, doi: 10.1080/00295639.2022.2027737.
- [16] Q. Tan, C. Qiu, J. Huang, Y. Yin, X. Zhang, and H. Liu, "Path tracking control strategy for off-road 4WS4WD vehicle based on robust model predictive control," *Robotics and Autonomous Systems*, vol. 158, p. 104267, Sep. 2022, doi: 10.1016/j.robot.2022.104267.
- [17] L. E. J. Alkurawy and K. G. Mohammed, "Model predictive control of magnetic levitation system," *International Journal of Electrical and Computer Engineering (IJECE)*, vol. 10, no. 6, pp. 5802-5812, Dec. 2020, doi: 10.11591/ijece.v10i6.pp5802-5812
- [18] N. Krausch et al., "High-throughput screening of optimal process conditions using model predictive control," *Biotechnology and Bioengineering*, Sep. 2022, doi: 10.1002/bit.28236.





- [19] Y. A. Elthokaby, I. Abdelsalam, N. Abdel-Rahim, and I. M. Abdealqawee, "Model-predictive control based on Harris Hawks optimization for split-source inverter," *Bulletin of Electrical Engineering Informatics (BEEI)*, vol. 11, no. 4, pp. 2348-2358, Aug. 2022, doi: 10.11591/eei.v11i4.3823.
- [20] A. K. Kojouri and J. M. Fard, "An efficient application of particle swarm optimization in model predictive control of constrained two-tank system," *International Journal of Electrical and Computer Engineering (IJECE)*, vol. 12, no. 4, pp. 3540-3550, Aug. 2022, doi: 10.11591/ijece.v12i4.pp3540-3550.
- [21] Y. Jiang, Z. Peng, C. Meng, L. Liu, D. Wang, and T. Li, "Data-driven finite control set model predictive speed control of an autonomous surface vehicle subject to fully unknown kinetics and propulsion dynamics," *Ocean Engineering*, vol. 264, p. 112474, Nov. 2022, doi: 10.1016/j.oceaneng.2022.112474.
- [22] M. Gopal, "Signal processing in digital control," in *Digital control and state variable methods: Conventional and intelligent control systems*, S. Jha, K. Ghosh, N. Kapoor, Eds., 4th ed., New Delhi, India: McGraw-Hill Education Pvt. Ltd., 2012, pp. 21-118.
- [23] J. Liu, L. Sun, W. Tan, X. Liu, and G. Li, "Finite time observer based incremental nonlinear fault-tolerant flight control," *Aerospace Science and Technology*, vol. 104, p. 105986, Sep. 2020, doi: 10.1016/j.ast.2020.105986.
- [24] J. Huang, H. An, Y. Yang, C. Wu, Q. Wei, and H. Ma, "Model predictive trajectory tracking control of electro-hydraulic actuator in legged robot with multi-scale online estimator," in *IEEE Access*, vol. 8, pp. 95918-95933, May 2020, doi: 10.1109/ACCESS.2020.2995701.
- [25] A. Laddha, A. Hazra, and M. Basu, "Power production strategies from renewable energy resources in a hospital campus considering economic aspect," *2016 IEEE 7th Power India International Conference (PIICON)*, 2016, pp. 1-6, doi: 10.1109/POW-ERI.2016.8077282.

BIOGRAPHIES OF AUTHORS







Ashish Laddha     completed B.E. degree (Electrical Engineering) from College of Technology and Engineering (MPUAT), Udaipur, India in 2012. He pursued the M.E. (Power Engineering) from Faculty Council of Engineering & Technology, Jadavpur University, Kolkata, India in 2015. Recently, he submitted Ph.D. thesis (Electrical Engineering) at the Malaviya National Institute of Technology, Jaipur, India. His areas of interests are the model prediction-based control, meta-heuristic optimizers, hybrid distributed generation, dc/dc converters, and generation scheduling. He can be contacted at email: 2016ree9538@mnit.ac.in.



Satyanarayana Neeli     completed his B.Tech. from Jawaharlal Nehru Technological University, Hyderabad, India in 2000. He obtained the M.E. (Control Systems Engineering) from Andhra University College of Engineering, Visakhapatnam, India in 2004. He did Ph.D. (System and Control Engineering) from Indian Institute of Technology, Delhi, India in 2014. Currently, he is an Assistant Professor in the Department of Electrical Engineering, Malaviya National Institute of Technology, Jaipur, India since 2015. His research fields are predictive control, optimal control, nonlinear control systems, control of uncertain systems, discrete time systems, design of observers and its control applications, estimation, and stability of time-delayed systems. He can be contacted at email: nsnarayana.ee@mnit.ac.in.



Vijayakumar Krishnasamy     pursued graduation in Electrical and Electronics Engineering from Coimbatore Institute of Technology (CIT), which is located in an Indian city Coimbatore (in the year 2006). Afterward, he completed M.Tech in the year 2009 from National Institute of Technology of the Tiruchirappalli district of the Indian sub continent. Subsequently, he obtained Ph.D. from the same institute in the year 2012. Later, he worked at the Nanyang Technological University (NTU) of the Singapore from 12-2012 to 12-2013. He worked as an Assistant Professor in the Department of Electrical Engineering, Malaviya National Institute of Technology, Jaipur, India from 2013 to 2018. He has been working as an Assistant Professor at the School of Electrical and Computer Engineering, Indian Institute of Information Technology, Design and Manufacturing, Kancheepuram, Chennai, India since 2018. His research interests are embedded controllers, internet of things, renewable energy systems, smart grid, home energy management system, power and industrial electronics. He can be contacted at email: vijayakumar@iiitdm.ac.in.